Liquid Crystals
Publication details, including instructions for authors and subscription information:
http://www.informaworld.com/smpp/title~content=t713926090

Chiral nematic liquid crystals in cylindrical cavities. A classification of planar structures and models of non-singular disclination lines

J. Bezić[a]; S. Žumer[a]
[a] Physics Department, University of Ljubljana, Ljubljana, Slovenia

To cite this Article Bezić, J. and Žumer, S.(1993) 'Chiral nematic liquid crystals in cylindrical cavities. A classification of planar structures and models of non-singular disclination lines', Liquid Crystals, 14: 6, 1695 — 1713
To link to this Article: DOI: 10.1080/02678299308027709
URL: http://dx.doi.org/10.1080/02678299308027709

LIQUID CRYSTALS, 1993, VOL. 14, NO. 6, 1695–1713

Chiral nematic liquid crystals in cylindrical cavities

A classification of planar structures and models of non-singular disclination lines

by J. BEZIĆ† and S. ŽUMER*

Physics Department, University of Ljubljana,
Jadranska 19, 61111 Ljubljana, Slovenia

A part of homotopy theory is applied to classify planar structures in chiral nematic liquid crystals confined to cylindrical cavities. The resulting classification is exact in the approximation of undeformed chiral nematic surfaces. Within this approach the relative stability of possible planar structures with surface and bulk disclination lines is discussed. The number and the shape of these disclinations, which in some cases form spiral structures, are predicted. Further approximate analytical expressions for non-singular director fields close to disclination lines with integral strength are introduced. Our predictions, which are also in agreement with some previously suggested pictures of such director fields, are used to improve stability considerations of the confined planar chiral nematic structures in tubes and droplets.

1. Introduction

Here we are going to discuss restricted chiral nematic phases with planar chiral nematic surfaces [1]. Observations of polymer dispersed chiral nematic (N*) droplets with planar anchoring conditions [2, 3] showed that in N* phases with negative dielectric anisotropy, the applied electric field stabilizes planar structures. In the experiment with N* phases confined to tubes [1], the anchoring was homeotropic. Planar structures were obtained after a phase transition from a smectic A phase to the N* phase. In tubes, more disclination lines were observed than in droplets. Furthermore, the observation of structures in tubes shows the difference between singular and non-singular (escaped) director fields around disclination lines.

Within the homotopy theory, it was shown [4] that in the N* phase only disclination lines, but not point defects, are possible. The description of these disclination lines is consistent with a classification of N* disclination lines into three classes [5, 6]. Only two of them: χ and λ disclination lines are considered in this contribution. χ disclination lines are singular in the director field $\mathbf{n}$, but are not singular in the field corresponding to local directions of the helical axes. λ disclination lines are singular in the field of helical axes but are non-singular in the director field [4–6]. From the topological point of view, there is one χ disclination line for every integer and half integer: $0, +1/2, -1/2, +1, -1, +3/2, -3/2, +2, \ldots$. These numbers (denoted by the letter s) are called strengths of the disclination lines. The χ disclination lines can be

* Author for correspondence.
† Deceased 5 February 1993.

0267–8292/93 $10·00

combined using the summation rules for the line strength numbers. (The relationship (mapping) between the listed numbers and χ disclination lines is usually referred to as an isomorphism.) From the topological point of view, there are also many λ disclination lines, but in our model structures, only $+1/2$ and $-1/2$ λ disclination lines can be found. These two λ disclination lines are the most common and in [5] and [6] are called $+\lambda$ and $-\lambda$, respectively.

If there are only χ disclination lines present, the N* surfaces are everywhere well defined (non-degenerate N* surfaces) with the director field everywhere tangential to them and with the helical axis as a local normal. Therefore, such a director field can be described as a two dimensional (2D) nematic. In the case of an undeformed N* phase, the N* surfaces are planes and the director field in these planes is homogeneous.

The structures singular in director fields are energetically demanding, as was shown for nematic structures [7], therefore close to χ disclination lines, structures with non-singular director fields (escaped structures) may be more stable. As follows from the homotopy theory [4, 8], the escape is possible for disclination lines of integral strength. For disclination lines, where strength is a multiple of 2, a structure non-singular in either director field or helical axis field was predicted, but no model structure was proposed [4, 8]. Qualitative pictures of some χ disclination lines with non-singular director field are presented in [6, 9, 10].

In § 2 of this contribution, we first model the possible 2D nematic strcutures which can occur in non-degenerate N* surfaces. Next, in § 3, using symmetry arguments similar to those used in [11] for disclination lines in nematic phases, we construct a three dimensional planar N* structure confined to a cylindrical tube. In § 4, we try to improve results obtained in the approximation of non-degenerate N* surfaces by introducing escaped cores for χ disclination lines. Examples of structures constructed following the steps described in § 2–4 are presented in § 5. In § 6, we discuss our results, compare them with available experimental results and underline the similarity between planar structures in droplets and tubes.

2. Nematic circles with strong anchoring on the circumference

In the homotopy theory, disclination lines in a three dimensional space and point defects in a two dimensional space are classified by encircling them with loops [12] and mapping them into an order parameter space [8]. Maps of loops are again loops or curves connecting equivalent points in the order parameter space. The 2D nematic phase is usually given as a straightforward example for homotopy groups [8]. Taking into account the $\mathbf{n} = -\mathbf{n}$ symmetry of the director fields, we find that its group of point defects is isomorphic to integers

$$\pi_1(P^1) \simeq Z. \tag{1}$$

The space P^1 is the circumference of a circle with radius equal to one and with opposite points of the circumference identified (see figure 1 (*a*)). $\pi_1(P^1)$, the first homotopy group of the 2D nematic phase, is therefore the group of curves on the circumference. Some examples with corresponding defect strengths are: a curve connecting two opposite points ($s = 1/2$) (see figure 1 (*c*)), a curve connecting a point with itself ($s = 1$) (see figure 1 (*b*)) and a curve winding once around the circle and thereafter ending in a point opposite to its starting point for $s = 3/2$. All these curves must be drawn in the positive direction [8]; that is, curves of equal length drawn in the opposite direction correspond to defects with negative strength.

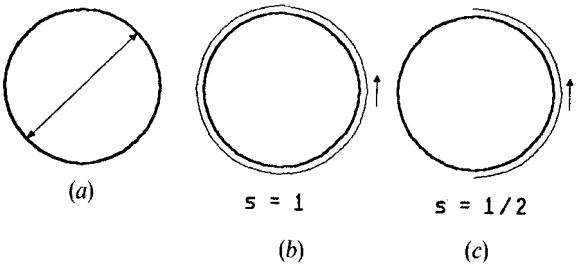

Figure 1. (*a*) The P^1 space representing all possible orientations of the director **n** in the 2D nematic. The arrow connects a pair of identified opposite points. (*b*) The curve connecting a point with itself, representing the $s=1$ defect. (*c*) The curve connecting a pair of opposite points, representing the $s=1/2$ defect.

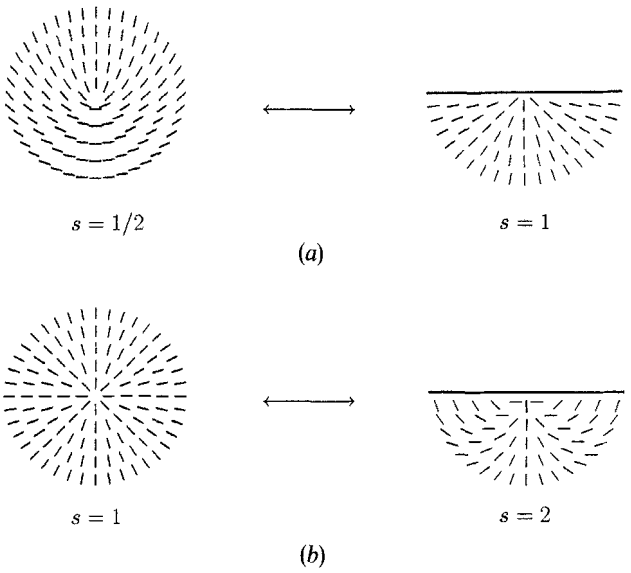

Figure 2. Two pairs of corresponding bulk and surface defects. The similarity of the director field around bulk and surface $s=1$ defects can be seen. (*a*) The pair of $s=1/2$ bulk and $s=1$ surface defects—parallel anchoring. (*b*) The pair of $s=1$ bulk and $s=2$ surface defects—homeotropic anchoring.

The above conclusions are valid for defects in the bulk of a 2D nematic phase; that is, only defects in the bulk can be completely surrounded by a curve forming a loop (for examples of surface and bulk defects see figure 2). Defects on the surface can be surrounded only on the nematic side of the surface, that is from one point to the other point of the surface [13, 14]. In the case of strong anchoring, there is only one orientation of the director at the surface allowed, and therefore both points on the curve which begin and end on the surface are mapped either into one point of into two opposite points on the circumference. Thus the curves connecting surface points of a 2D nematic are curves on the circumference P^1 corresponding to a first homotopic group. So we conclude that in the case of strong anchoring any surface defect can be

transformed into a corresponding bulk defect and vice versa (see figure 2). The only difference between a surface defect and a corresponding bulk defect is their strength. While the defect is moved to the surface, the surrounding director field is compressed so that the surface defect has twice the strength of the bulk defect but occupies only half its volume. In figure 2 there are two pairs of defects illustrating this effect for parallel and homeotropic surface anchoring. A bulk defect with strength $s=1/2$ is transformed into a surface defect with strength $s=1$, and a bulk defect with strength $s=1$ is transformed into a surface defect with strength $s=2$. In these special cases given in figure 2 around both the surface $s=1$ defect and the bulk $s=1$ defect, there is a radial structure.

The described equivalence of surface and bulk defects cannot be taken for granted. A counter-example can be found with defects in the polarization vector **p** in the smectic C* phase. The space P^1 of the 2D director must be substituted by S^1, which is the circumference of a unit circle with no points identified. Where only one direction of the polarization vector **p** is allowed at the surface, the statement for the director **n** must be modified. As a result, allowed bulk defect strengths $+1, -1, +2, -2, +3, -3, \ldots$ and surface defect strengths $+2, -2, +4, -4, +6, -6, \ldots$ are obtained. But in the case where on the surface both directions **p** and $-\mathbf{p}$ are possible (as in chevrons [15]) there are additional surface defect strengths $+1, -1, +3, -3, +5, -5, \ldots$ allowed. None of these additional surface defects (disclinations) has a corresponding bulk defect (disclination), because bulk defects with strengths $+1/2, -1/2, +3/2, -3/2, +5/2, -5/2, \ldots$ are not allowed for any vector field.

Using the equivalence of surface and bulk defects, the possible structures of a 2D nematic phase with strong anchoring on its 'surface' can be classified. Each structure is defined by defects occurring in the director field. In the case of uniform anchoring (along the circumference, the anchoring axis does not change its orientation relative to the surface normal), the director field on the circumference is mapped into a curve connecting a point with itself ($s=1$) on P^1. Therefore the sum of bulk defect strengths, if there are no surface defects, is equal to one

$$\sum_i s_i^{\text{bulk}} = 1. \tag{2a}$$

According to our definition the strength of any defect that moves from the bulk to the surface is multiplied by two. Thus in the case of combined bulk and surface defects the expression (2*a*) is generalized

$$\sum_i s_i^{\text{bulk}} + (1/2)\sum_j s_j^{\text{surface}} = 1, \tag{2b}$$

(for illustrations see figure 3) or in the case of N holes in the 2D nematic phase with strong parallel anchoring on their circumference

$$\sum_i s_i^{\text{bulk}} + (1/2)\sum_j s_j^{\text{surface}} = 1 - N. \tag{2c}$$

The expression could be also easily generalized to a non-uniform surface of arbitrary shape with varying angle between surface normal and the anchoring axis. The only limitation is strong anchoring.

It is known that the free energy of a point defect in a bulk is proportional to the square of its strength [5]. The same is true for surface defects. That is, when a defect is moved to the surface, the derivatives of the director field are multiplied by two and so is

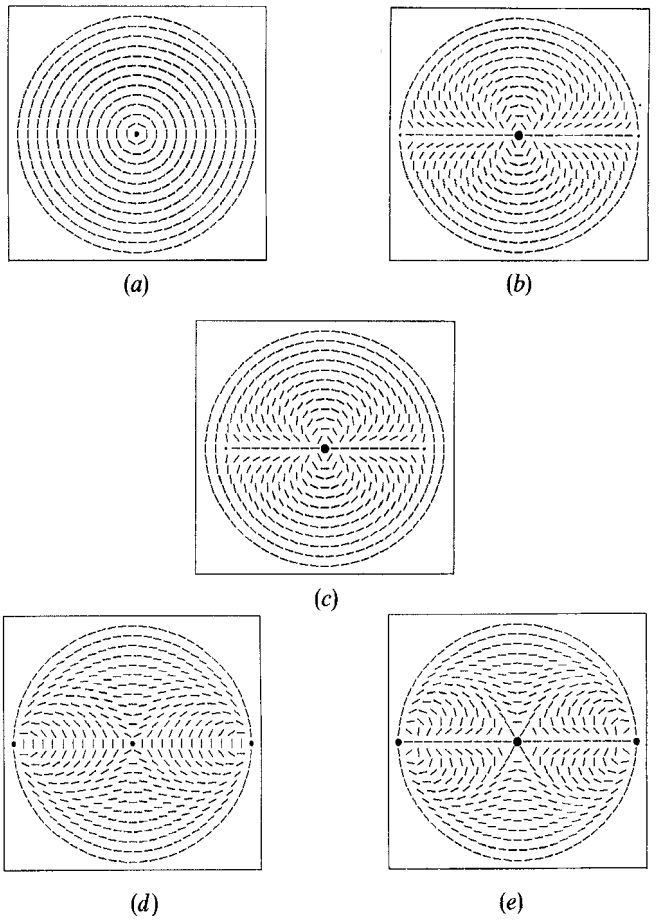

Figure 3. Five combinations of bulk and surface defects in a circle with tangential boundary conditions. The positions of defects are marked with black circles with radii proportional to bulk defect strengths. Using the same description as in expression (2*d*), the combinations are: (*a*) (1;), (*b*) (−2; 3, 3), (*c*) (−1; 2, 2), (*d*) (2, −1/2, −1/2;), and (*e*) (2; −1, −1).

the defect strength. On the other hand, the size of the space occupied by surface defects is only half of the size corresponding to bulk defects (see figure 2). The free energy of a structure with point defects is thus approximately proportional to the sum of the squares of defect strengths

$$\left(\sum_i s_i^{\text{bulk}}\right)^2 + (1/2)\left(\sum_j s_j^{\text{surface}}\right)^2, \tag{3a}$$

where one half in front of the second sum reflects the difference between the two kinds of defect. To predict the most stable structures, we choose those allowed combinations with the lowest sum of defect strength squares. Such combinations are

$$(1/2, 1/2;),\ (;1, 1),\ (-1/2, 1/2, 1/2, 1/2;),\ (-1/2; 1, 1, 1),$$
$$(1;),\ (;2),\ (-1, 1/2, 1/2, 1/2, 1/2),\ (-1; 1, 1, 1, 1),\ (-1, 1, 1;),\ (-1; 2, 2),\ (2, -1/2, -1/2;),$$
$$(2; -1, -1),\ (1, 1, -1/2, -1/2;),\ (1, 1; -1, -1), \ldots, \tag{3b}$$

where defect strengths before the semicolon belong to bulk defects and those after the semicolon belong to surface defects. The values of the free energy of these structures are proportional to

$$0{\cdot}5,\ 1,\ 1,\ 1{\cdot}75,\ 1,\ 2,\ 2,\ 3,\ 3,\ 5,\ 4{\cdot}5,\ 5,\ 2{\cdot}5,\ 3,\ldots, \tag{3c}$$

respectively. The first two combinations are variations of the planar bipolar structure and the fourth and the fifth are variations of the planar monopolar structure [16]. Some of the presented combinations will be useful for the description of planar N* structures in tubes and some of them are presented in figure 3.

3. χ disclination lines in planar chiral nematic structures

In the case of planar structures confined to droplets and tubes the confining surface cuts circles out of N* planes. In each circle, there is a 2D nematic director field which can, in the approximation of non-degenerate N* surfaces, be described according to the above predictions. The whole N* structure within a tube can thus be constructed by simply making a stack of relatively rotated 2D structures. Such a rotation satisfies the boundary conditions for the director field and in the largest possible part of the tube realizes the intrinsic N* twist. Depending on the symmetry of the initial 2D structure, the formation of the N* twist is expected to induce deformations in this 2D structure.

Let us try to obtain a formal description of the above construction. We first introduce the required quantities: $\mathbf{n}(\mathbf{r})$—the orientation of the director at the point with position vector $\mathbf{r}$ and $\mathbf{R}(\varphi_0)$ is the rotation matrix for an angle φ_0 around the z axis, which is also the symmetry axis of the tube. All quantities of the 2D nematic have the abbreviation 'nem' as a subscript. To rotate a 2D nematic structure in a N* plane through an angle φ_0, the coordinate system must first be rotated through this angle that is equivalent to the rotation of the position vector for the angle $-\varphi_0$

$$\mathbf{R}(-\varphi_0)\mathbf{r}, \tag{4a}$$

then the director field is evaluated in this rotated coordinate system

$$\mathbf{n}_{\mathrm{nem}}(\mathbf{R}(-\varphi_0)\mathbf{r}) \tag{4b}$$

and the resulting director field is transformed back to the original coordinate system

$$\mathbf{R}(\varphi_0)\mathbf{n}_{\mathrm{nem}}(\mathbf{R}(-\varphi_0)\mathbf{r}). \tag{4c}$$

A formal description of the above construction is thus

$$\mathbf{n}(\mathbf{r}) = \mathbf{R}(\varphi_0)\mathbf{n}_{\mathrm{nem}}(\mathbf{R}(-\varphi_0)\mathbf{r}), \tag{4d}$$

where φ_0 must, close to the z axis, satisfy the condition that the twist of the director field from one N* plane to the other is the intrinsic N* twist qz defined by the N* wave number q. Along the symmetry axis of the tube (the z axis) there is either a χ disclination line with strength s_0, or there is no disclination in the case of $s_0 = 0$.

In the first step we limit our description to the vicinity of the z axis where we can neglect the effect of the surface constraints given by the expression (2 b) and describe the director field of the 2D nematic as a linear combination of the coordinate vectors $\mathbf{e}_x$ and $\mathbf{e}_y$ with Ω_{nem} being the angle between the director $\mathbf{n}_{\mathrm{nem}}$ and the x axis of the chosen cartesian coordinate system [11]

$$\mathbf{n}_{\mathrm{nem}} = \cos\Omega_{\mathrm{nem}}\mathbf{e}_x + \sin\Omega_{\mathrm{nem}}\mathbf{e}_y \tag{5a}$$

$$\Omega_{\mathrm{nem}} = s_0\varphi + \Omega_0. \tag{5b}$$

Here the angle Ω_0 is a constant and

$$\varphi = \arctan(y/x) \tag{5c}$$

is the polar angle in the cylindrical coordinate system measured with respect to the x axis of the cartesian coordinate system. Using expressions (4) the N* planar structure close to the centre of the tube is expressed as

$$\mathbf{n} = \cos\Omega \mathbf{e}_x + \sin\Omega \mathbf{e}_y, \tag{6a}$$

$$\Omega = s_0(\varphi - \varphi_0) + \varphi_0 + \Omega_0. \tag{6b}$$

The difference between Ω_{nem} and Ω must be equal to the intrinsic N* twist

$$\Omega - \Omega_{nem} = qz. \tag{7a}$$

By substituting expressions (5) and (6 b) into expression (7 a), a condition for angle φ_0 is obtained

$$(1 - s_0)\varphi_0 = qz. \tag{7b}$$

For $s_0 \neq 1$ the condition (7 b) can be rewritten as

$$\varphi_0 = qz/(1 - s_0) \quad \text{for} \quad s_0 \neq 1. \tag{8a}$$

For $s_0 = 1$, the structure is axially symmetric around the z axis so that condition (7 b) cannot be satisfied. Therefore, for a $s_0 = 1$ disclination line at the tube axis, no N* twist can be formed by rotating the 2D nematic structure from one N* plane to the other N* plane. Thus, the $s_0 = 1$ disclination line must be displaced so that there is no disclination line along the tube axis similarly as in the $s_0 = 0$ case. The expression

$$\varphi_0 = qz \quad \text{for displaced} \quad s_0 = 1 \tag{8b}$$

is not a solution of condition (7 b) for $s_0 = 1$, but for $s_0 = 0$, reflecting the fact that there is no disclination line at the tube axis. For $s_0 \neq 1$, substituting our approximate solutions for the rotation of the N* structure (expression (8 a)) back into expression (6), the well-known expressions for χ disclination lines along the z axes (or the undeformed N* phase structure for $s_0 = 0$) are reproduced [5, 6].

Let us now find a way to satisfy the surface constraints described by expression (2 b). For cases corresponding to $s_0 \neq 1$, with (or without) a disclination line along the z axis, additional disclination lines must be added to the central disclination line. The positions of these additional disclination lines must be consistent with the symmetry of the central disclination line. Therefore, these additional disclination lines are $s = +1/2$ and $s = -1/2$ bulk disclination lines or $s = +1$ and $s = -1$ surface disclination lines, as will be shown using expressions (9)–(11). In expression (9), the symmetry of disclination lines with strength s_0 is expressed in terms of rotation angles ψ_0 that leave the structure unchanged

$$\mathbf{n}(\mathbf{r}) = \mathbf{R}(\psi_0)\mathbf{n}(\mathbf{R}(-\psi_0)\mathbf{r}). \tag{9}$$

Using the ansatz (6 a), we find that the difference between the angle Ω on the left hand side and the angle Ω on the right hand side of expression (9) must be a multiple of π. Thus, an expression for the angle ψ_0 is

$$s_0\varphi + qz + k\pi = s_0(\varphi - \psi_0) + \psi_0 + qz, \quad k = 0, +1, -1, +2, -2, \ldots \tag{10a}$$

and the angle ψ_0 is for $s_0 \neq 1$ given by

$$\psi_0 = k\pi/|1 - s_0|, \quad s_0 \neq 1. \tag{10b}$$

The smallest non-zero ψ_0 that preserves the disclination line (with strength s_0) unchanged is obtained for $k=1$. Therefore, the number of additional disclination lines of equal strength needed to preserve the symmetry of a disclination line with strength $s_0 \neq 1$ is

$$M = 2\pi/\psi_0(k=1) = 2|1-s_0|. \tag{10d}$$

If additional disclination lines are bulk disclination lines; using the expressions (2*b*) and (10*d*) we find that their strength s is

$$s = (1-s_0)/(2|1-s_0|) = +1/2, \ -1/2, \tag{11}$$

and similarly, if they are surface disclination lines their strength is either $+1$ or -1. Two examples, $s_0=0$ and $s_0=2$ will be discussed in detail in § 5 (see figures 6 and 8), as well as more exotic cases with $s_0=-1$ and $-1/2$ (see figures 9 and 10 of § 5).

For the $s_0=1$ central disclination line, we find that $M=0$ directly from expression (2*b*). The corresponding structure, where the central disclination line is displaced from the centre towards the surface and twisted (see expression (8*b*)) is in figure 7.

The allowed structures in spherical droplets are very similar to the structures in tubes. In addition to the rotation of 2D nematic circles needed in tubes, the contraction of these director fields towards the poles of droplets, where circles converge to points, is needed.

4. Disclination lines of integral strength. Non-singular director fields

As was shown in [17], the non-singular cores for χ disclination lines can be reasonably well-described by a director field obtained by an approximate minimization of the Frank free energy. Here we briefly repeat the evaluation, so that we will be able to show how the λ disclination lines appear. The first step in the minimization is the description of the director field around χ disclination lines, using our approximation of non-degenerate N* surfaces. In cylindrical coordinates we find

$$\mathbf{n} = \cos\Omega \mathbf{e}_\rho + \sin\Omega \mathbf{e}_\varphi,$$

with

$$\Omega = (s_0-1)\varphi + qz + \Omega_0. \tag{12}$$

Here, the expression for the Ω differs from expression (6) because of the transition from a cartesian to a cylindrical coordinate system.

In the second step, the angle Ψ is added (see figure 4) to enable the tilt of the director out of the N* planes

$$\mathbf{n} = \cos\Omega \sin\Psi \mathbf{e}_\rho + \sin\Omega \sin\Psi \mathbf{e}_\varphi + \cos\Psi \mathbf{e}_z. \tag{13}$$

This ansatz is then substituted into the Frank free energy. To simplify the resulting expression for free energy, the free energy is integrated over cylindrical coordinates φ and z and minimized over Ψ as a function of ρ to obtain

$$\rho/r^e_{s_0} = (\tan(\Psi/2))^{1/|s_0|}. \tag{14}$$

In expression (14), s_0 is the strength of the χ disclination line and $r^e_{s_0}$ is the radius of the escaped core (upper index e for escaped). Two model structures ($s_0=1$ and 2), described by expressions (12)–(14), were first introduced in [17]. Here, we describe in detail

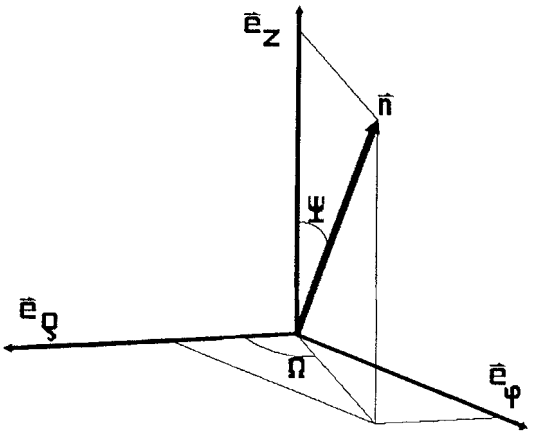

Figure 4. The angles Ω and Ψ of the director $\mathbf{n}$ in the cartesian coordinate system. Ψ is the angle between the z axis and the director and Ω is the angle of rotation around the z axis.

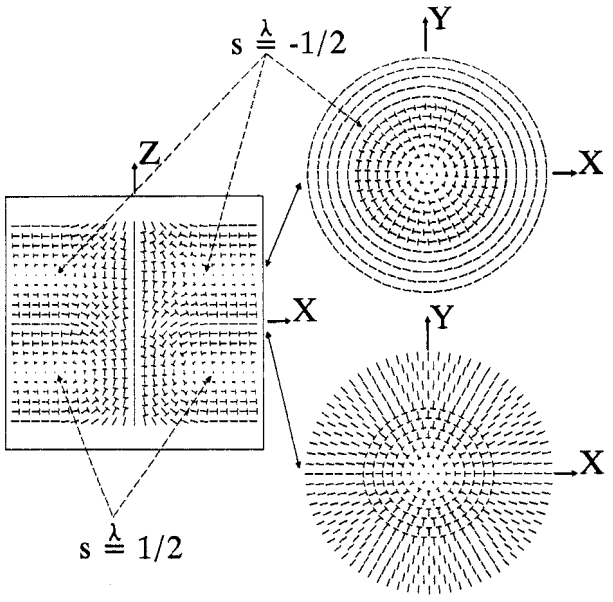

(*a*)

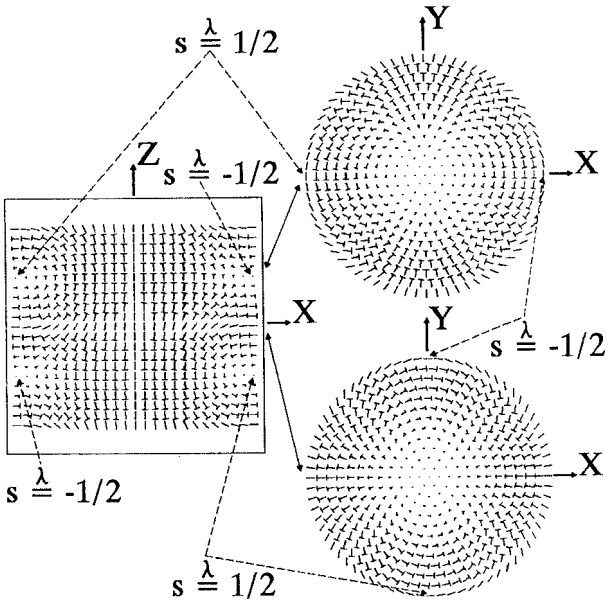

(*b*)

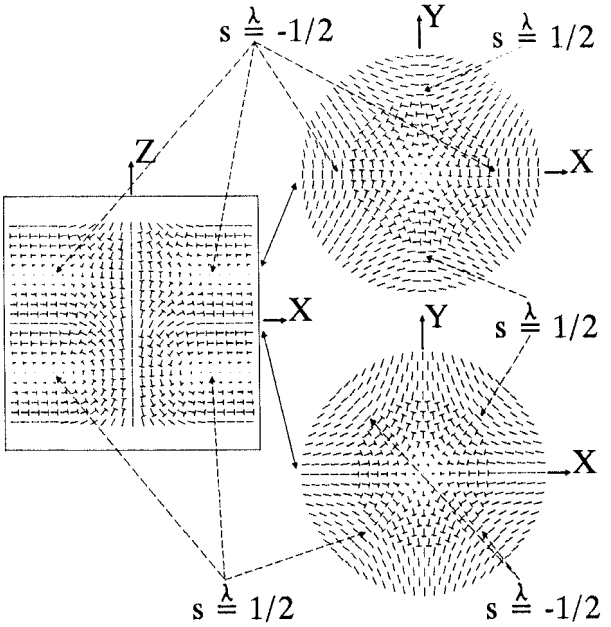

(*c*)

Figure 5. In director non-singular structures for χ disclination lines of strengths (*a*) $s=1$, (*b*) $s=-1$ and (*c*) $s=2$. In these figures the coordinate system is defined with the z axis parallel to the χ disclination line and x and y axes normal to this χ disclination line and parallel to the N* planes. The full lines with two arrow heads show where the (x, y) cross-section is cutting the (x, z) cross-section. Arrows with dashed lines are pointing at λ disclination lines. In the (x, z) cross-section points of the in director non-singular $+1/2$ and $-1/2$ λ disclination lines can be seen where the director is perpendicular to the (x, z) plane. In the (x, y) cross-sections, points of these λ disclination lines can be seen where the molecular director is normal to the radial direction.

examples of the χ disclination line with $s_0 = 1$, 2 and -1. In figure 5 there are one x–z and two x–y cross-sections for each case calculated using expressions (12)–(14). The z axes are those along χ disclination lines. Out of plane director field is represented by 'mails' [5, 17]. Several common features of escaped structures can be observed.

(i) First, at the centre of each escaped structure the director field is everywhere parallel to the z axis.

(ii) Second, in the region where N* planes become degenerate, that is where the director field tilts out of the N* planes (which are parallel to the x–y plane), the $+1/2$ and $-1/2$ λ disclination lines appear. These λ disclination lines wind around the z axis and cross the x–z plane in the last point on the N* plane where the director is still parallel to the $\mathbf{e}_\varphi$ unit vector ($\Psi = \pi/2$ and $\Omega = \pi/2$, see also figure 4). On each x–z cross-section presented in figure 5, there are four such points. On the right hand side of the x–z cross-section, the lower point corresponds to the $+1/2$ λ disclination line and the upper one to the $-1/2$ λ disclination line.

(iii) The third common feature of escaped structures is that the number and the form of λ disclination lines depends on the symmetry of χ disclination lines.

The $s_0 = 1$ χ disclination line is, as we have seen in § 3, a particular case which must be treated separately. In planar N* structures, confined to tubes, these disclination lines are not along the symmetry axis of the tube, but nevertheless they have local axial symmetry (see figure 5(*a*)). Therefore, λ disclination lines which encircle $s_0 = 1$ χ disclination lines are circular. These circles are localized in N* planes where the director field is concentric and coincides with the circular field lines with the smallest radius.

For cases with $s_0 \neq 1$, the angle φ_0 in expressions (8) gives the rotation of the director fields around χ disclination lines (z axes of the tube) as a function of the z coordinate. The expression (10 *b*) describes the symmetry of director fields surrounding the cores of χ disclination lines.

The $s_0 = -1$ ($\varphi_0 = qz/2$, $\psi_0 = k\,\pi/2$) structure (see figure 5(*b*)) rotates around the χ disclination line according to expression (8 *a*). Because the angle ψ_0 from expression (10 *b*) is a multiple of $\pi/2$, there are in each N* plane four points where a λ disclination line crosses the N* planes. Therefore, λ disclination lines form a fourfold spiral rotating in the same sense as the N* twist. The existence of four λ disclination lines obeys the symmetry of a χ disclination line, but because of the fact that two of these four lines are $+1/2$ and two are $-1/2$ λ disclination lines, the symmetry of the $s_0 = -1$ χ disclination line is broken.

The $s_0 = 2$ ($\varphi_0 = -qz$, $\psi_0 = k\pi$) structure (see figure 5(*c*)) is rotated in the opposite sense to the intrinsic N* twist, that is by an angle $\varphi_0 = -qz$. Because the angle ψ_0 from expression (10 *b*) is a multiple of π, there are in each N* plane two points where a λ disclination line crosses the N* plane. Thus, a pair of one $+1/2$ λ disclination line and one $-1/2$ λ disclination line forms a double spiral rotating in the sense opposite to the N* twist.

5. Examples of planar chiral nematic structures in tubes

Combining the results of § 3 and § 4, we are now able to calculate Ω and ψ approximately by suitably summing rotation angles of all contributing disclination lines (details will be published elsewhere). Simple planar N* structures confined to cylindrical cavities for $s_0 = 0$, 1, 2, -1 and $-1/2$ are shown in figures 6 to 10 in two versions with planar anchoring (*a*, *b*) and one with homeotropic anchoring (*c*). In the (*a*)

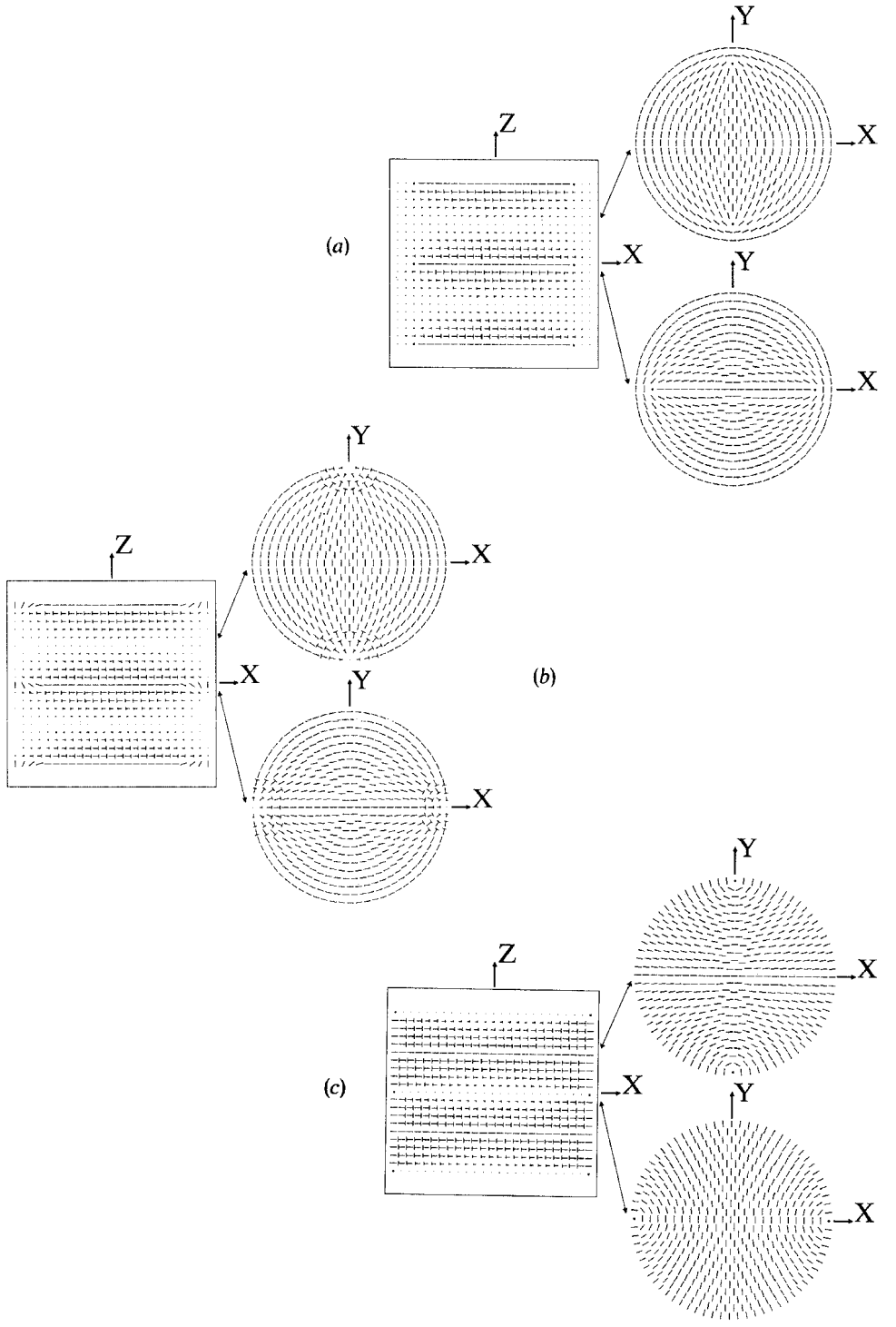

Figure 6. $s_0=0$. The structure with no central disclination line and two additional χ disclination lines with strength $s=1/2$ each. The director field in the two (x, y) cross-sections (*a*) and (*b*) is rotated through $+\pi/2$ from the lower to the upper cross-section. (For more general information on figures 6 to 10 see the beginning of § 5).

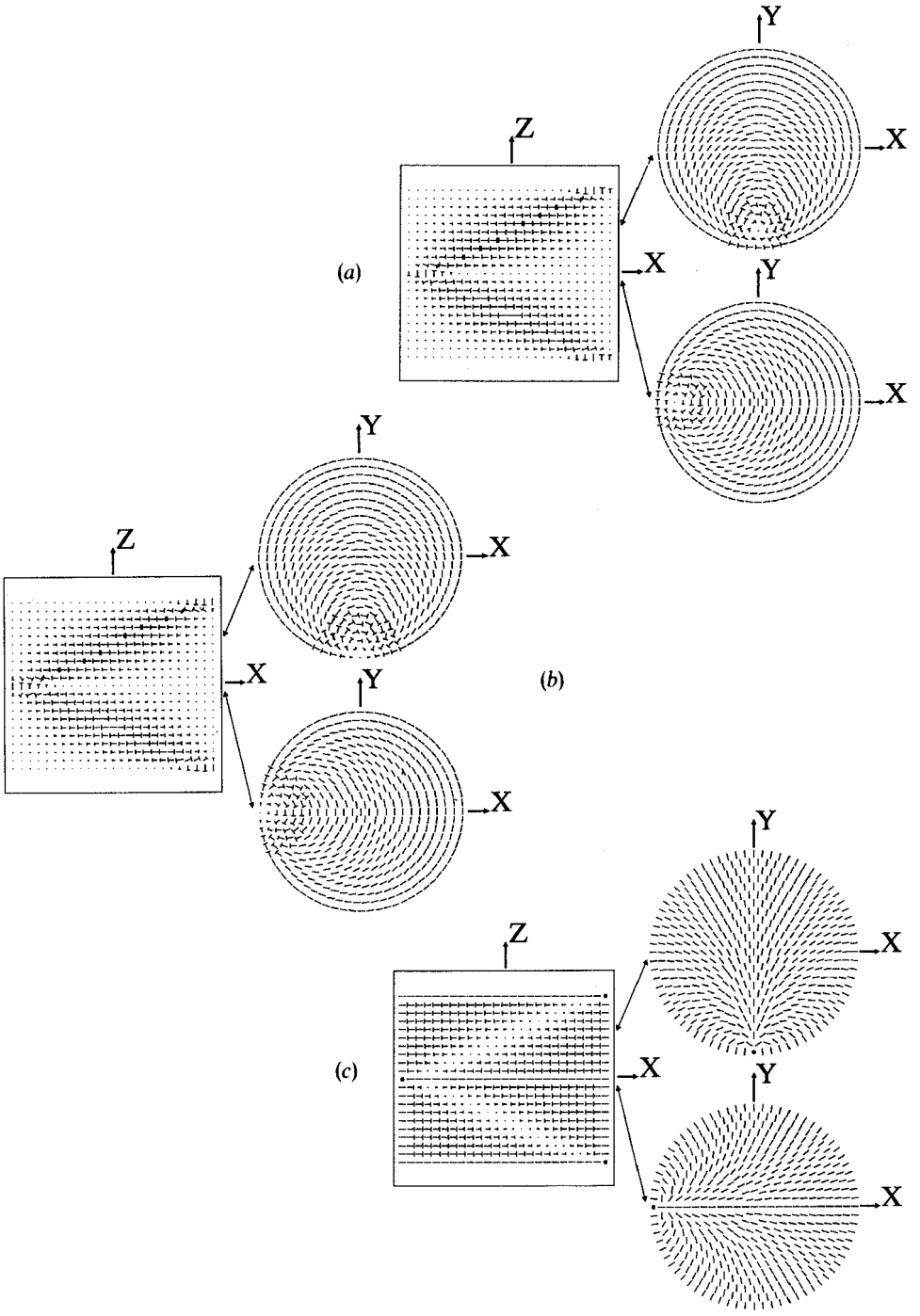

Figure 7. $s_0 = 1$. The structure with a displaced central disclination line and no additional χ disclination lines. In figure (*a*) the χ disclination line is in the bulk and non-singular. In figure (*b*), the anchoring is planar and the surface χ disclination line is non-singular. In figure (*c*) the anchoring is homeotropic and the surface χ disclination line is singular. The director field in the two (x, y) cross-sections is rotated through $+\pi/2$ from the lower to the upper cross-section.

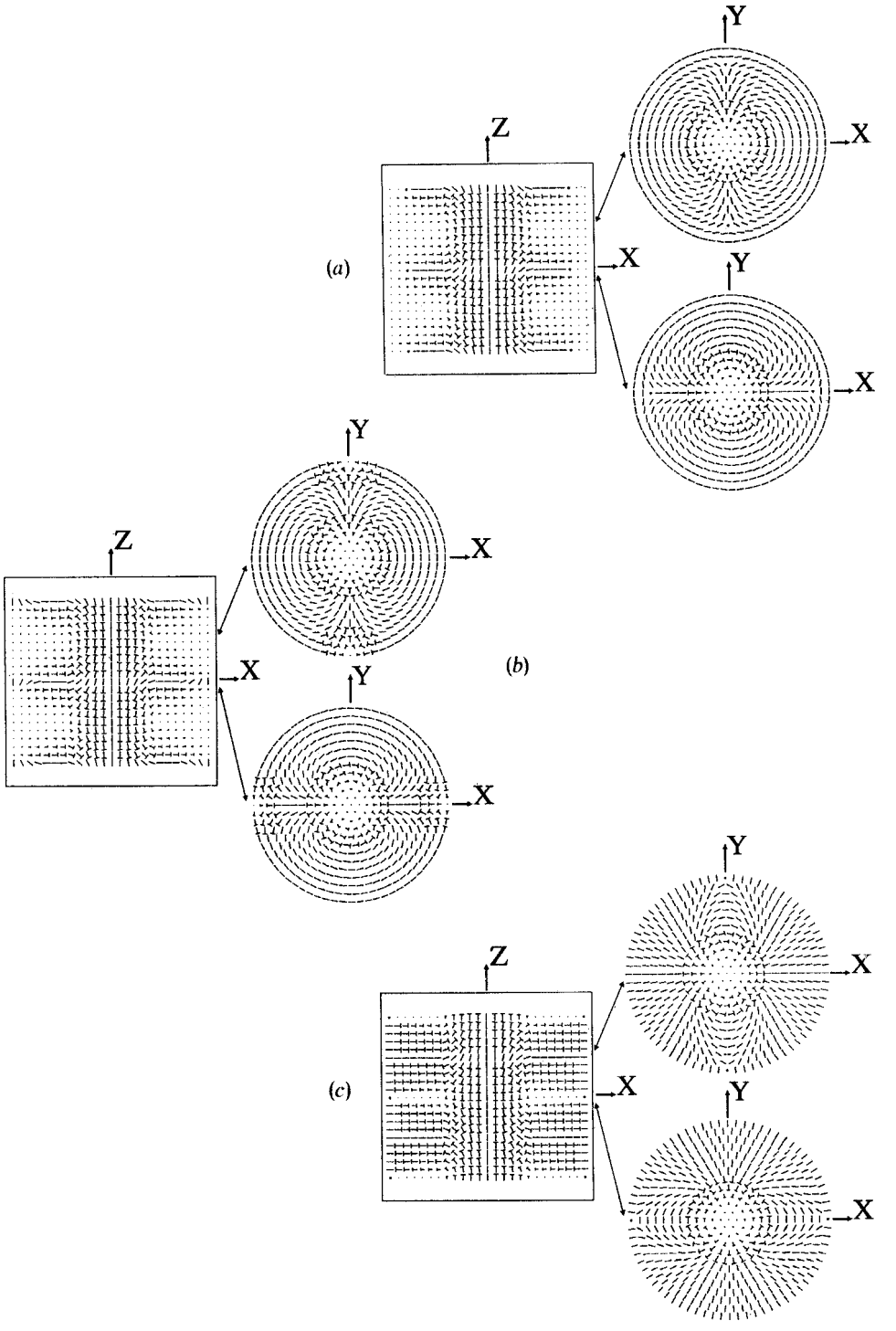

Figure 8. $s_0 = 2$. The structure with two additional χ disclination lines with strength $s = -1/2$ each. The central disclination line is non-singular in all three figures—(*a*), (*b*) and (*c*). The director field in the two (x, y) cross-sections is rotated through $-\pi/2$ from the lower to the upper cross-section.

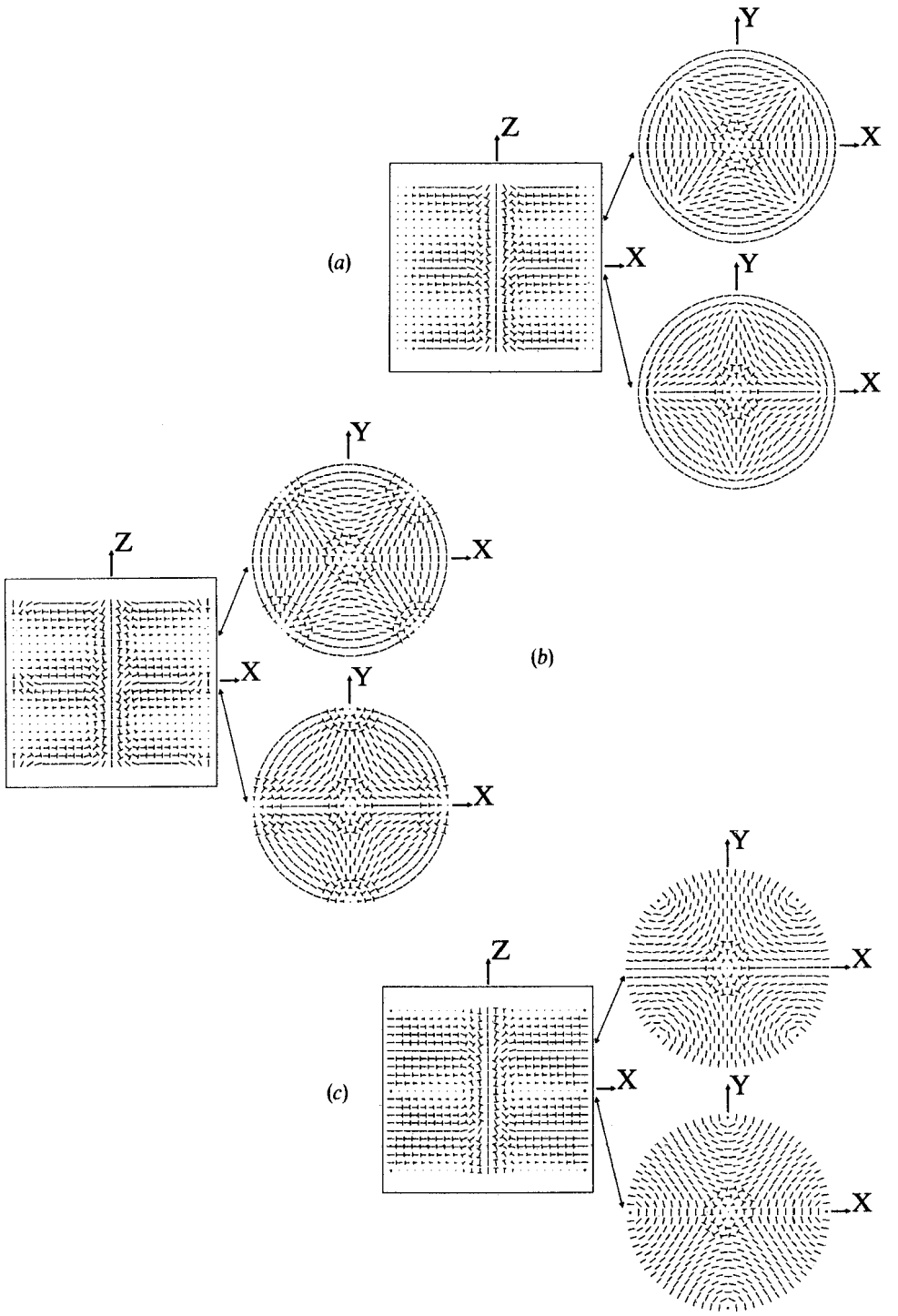

Figure 9. $s_0 = -1$. The structure with four additional χ disclination lines with strength $s = 1/2$ each. The central disclination line is non-singular in all three figures—(*a*), (*b*) and (*c*). The director field in the two (x, y) cross-sections is rotated through $+\pi/4$ from the lower to the upper cross-section.

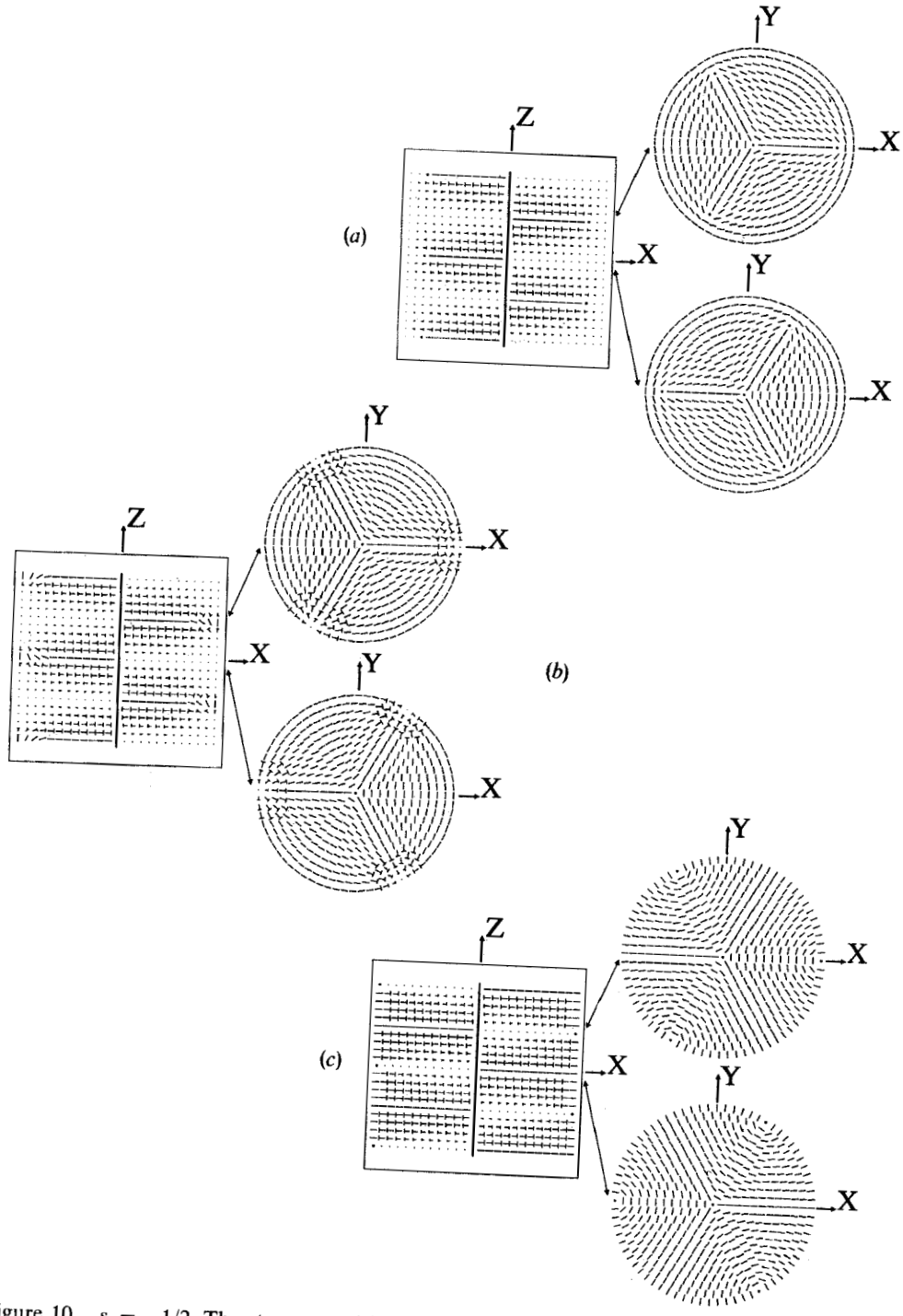

Figure 10. $s_0 = -1/2$. The structure with three additional χ disclination lines with strength $s = 1/2$ each. The central disclination line in all three figures—(*a*), (*b*) and (*c*) is singular and is marked with black points on the (x, y) cross-sections and with a thick line on the (x, z) cross-section. The director field on the two (x, y) cross-sections is rotated through $+\pi/3$ from the lower to the upper cross-section.

version, the additional χ disclination lines are bulk disclination lines, in the (*b*) and (*c*) versions the additional χ disclination lines are surface disclination lines. In the (*b*) versions, surface disclination lines can be non-singular in the director field, because the planar anchoring on the surface does not prevent the escape. In the (*c*) versions, surface disclination lines are singular, because the homeotropic anchoring prevents the escape. In all these figures, the z axis is along the tube axis and the x and y axes are normal to it. The full lines with two arrow heads are connecting pairs of lines parallel to the x axis: one on the (x, y) cross-section and one on the (x, z) cross-section. One such pair of cross-section lines represents one line in space. The (x, z) cross-section presents one N* pitch of the tube and the two (x, y) cross-sections are a quarter of the cholesteric pitch apart. Positions of singular χ disclination lines are marked with black points. The N* wave number is positive, and results in the right hand rotation of the director field.

The structure with $s_0 = 0$, which has no central disclination line ($\varphi_0 = qz$, $M = 2$, $s = 1/2$, see figure 6) is twisted through the same angle and in the same sense as the undeformed N* phase structure. The two additional χ ($s = 1/2$) disclination lines form a double spiral around the symmetry axis of the tube. If the two additional χ disclination lines are on the surface, they become $s = 1$ lines and for a planar surface anchoring (see figure 6 (*b*)), the director field around them is non-singular as described in § 4 (see figure 5 (*a*)).

As discussed in § 3, in the structure with $s_0 = 1$ ($\varphi_0 = qz$, $M = 0$, see figure 7), the central disclination line is displaced from the symmetry axis of the tube and there are no additional χ disclination lines. Since any structure around the $s_0 = 1$ disclination line is axially symmetric without external constraints, there are many different structures around such a line. Two director fields can be seen in figure 5 (*a*): the upper one is the concentric structure and the lower one is the radial structure. The concentric structure around the $s_0 = 1$ disclination line displaced from the tube axis can be seen in figures 7 (*a*) and (*b*) and a radial structure can be seen in figure 7 (*c*). At the tube axis, there is no disclination line, therefore the structure as a whole rotates as qz (see expression (8 *b*)). For planar anchoring, the χ disclination line either in the bulk (see figure 7 (*a*)) or on the surface (see figure 7 (*b*)) can have a non-singular director field. The same is true for homeotropic anchoring and the χ disclination line in the bulk, but for homeotropic anchoring and the χ disclination line on the surface, escape is not possible (see figure 7 (*c*)). With a χ disclination line on the surface, the director field is similar to the director field of the $s = 2$ bulk χ disclination line shown in figure 5 (*b*).

In the structure with $s_0 = 2$, there are three χ disclination lines ($\varphi_0 = -qz$, $M = 2$, $s = -1/2$, see figure 8). The central disclination line has strength $s_0 = 2$ with a possible non-singular director field. The structure as a whole rotates through the same angle, but in the opposite sense compared to the N* twist of the director field in an undeformed N* phase structure. The behaviour of additional $s = -1/2$ χ disclination lines is similar to the behaviour of additional χ disclination lines in the structure with no central disclination line ($s_0 = 0$). In the bulk (see figure 8 (*a*)) and in the case of homeotropic anchoring (see figure 8 (*c*)) they are singular, and on the surface in the case of planar anchoring (see figure 8 (*b*)) they are non-singular. On the surface, the director field around them is comparable with the director field around a bulk $s = -1$ χ disclination line as shown in figure 5 (*c*) and also in figure 9.

Comparing the free energy of structures allowed by symmetry (expressions (2 *d*) and (3 *b*)), two more structures are found to be quite stable: $s_0 = -1$ and $s_0 = -1/2$. In the structure with $s_0 = -1$ ($\varphi_0 = qz/2$, $M = 4$, $s = 1/2$, see figure 9), the director field of the central disclination line is non-singular and the four additional ($s = 1/2$) χ disclination

lines form a fourfold spiral rotating in the same sense as the N* twist of the director field in the undeformed phase, but with a half of its rate of rotation. In the structure with $s_0 = -1/2$ ($\varphi_0 = 3\,qz/2$, $M = 3$, $s = 1/2$, see figure 10) the singular central disclination line is surrounded by the three additional χ disclination lines forming a threefold spiral rotating in the same sense as the N* twist in the undeformed N* phase, but with a one and half times smaller rate. In both structures (with $s_0 = -1$ and with $s_0 = -1/2$ central disclination lines), the additional χ disclination lines behave in a similar way as in the $s_0 = 0$ case. That is, they have singular director fields in the bulk ($s = 1/2$) (see figures 9 (*a*) and 10 (*a*)) and can be non-singular if they are on the surface ($s = 1$) (see figures 9 (*b*) and (*c*), 10 (*b*) and 10 (*c*).

6. Discussion and comparison with experimental results [1–3]

This contribution is based almost entirely on geometry and symmetry arguments. The strong anchoring condition on the surface is used to determine possible 2D nematic defect combinations in circles cut from N* planes. The N* structures in tubes are reproduced by rotating 2D nematic structures so that the director field follows the intrinsic N* twist in the major part of the tube. As a result, we have N* structures without a straight χ disclination line at the symmetry axis of the tube for $s_0 = 0$ and 1, and with a straight line for all other values of s_0. For $s_0 \neq 1$, additional χ disclination lines spiralling around the symmetry axis of the tube are predicted. The main feature of these model structures, the spiralling of additional χ disclination lines, has been studied experimentally a long time ago [1], but no consistent theoretical explanation has been given. Particularly, the structure with no central disclination line ($s_0 = 0$) and the structure with a $s_0 = 2$ central disclination line with additional χ disclination lines rotating in the opposite sense compared to the twist of director field in the undeformed N* phase structure have been observed. Both structures were explained as combinations of χ disclination lines in agreement with our general model. Only the $s_0 = 2$ central disclination line was observed occasionally to split into two $s = 1$ χ disclination lines. This splitting does not break the symmetry of the $s_0 = 2$ structure and can be explained in the frame of symmetry arguments applied in this contribution. That is, the symmetry of the director field around a pair of $s = 1$ χ disclination lines is the same as the symmetry of the director field around a $s = 2$ χ disclination line.

Experimentally [1], some structures with many additional χ disclination lines were observed. These structures may be connected to our model structures with $s_0 = -1$ or $s_0 = -1/2$ central disclination lines, but the exact number of disclination lines has not been determined. What probably evades description by plain geometry and symmetry arguments are cases where additional straight χ disclination lines appear. In the literature [1], qualitative free energy arguments like a large bend elastic constant close to the N*–smectic A phase transition and the lengths of χ disclination lines are used to explain this phenomenon. Another interesting feature of χ disclination lines is the possibility of having a non-singular core, if their strength is an integer. An approximate minimization of the Frank free energy was performed in [17] and structures similar to model pictures presented in [6, 9, 10] were obtained. These structures are more stable than singular structures [17] and may explain the appearance of thick disclination lines observed experimentally [1]. The systems with planar anchoring can have the escaped director field in the core of the surface disclination lines as well (see figures 6 (*b*)–10 (*b*), but in the experiment homeotropic surface anchoring was used to stabilize the planar structure and no escape on the surface was possible (compare figures 6 (*c*)–10 (*c*)).

As already mentioned at the end of § 3, the planar structures in droplets are very similar to planar structures in tubes. Therefore, the model structures developed here can be modified [16] to describe planar structures in droplets [2, 3, 18]. Further models, also including gradual formation of planar structures with increasing external electric field, offering an explanation of the apparent absence of additional χ disclination lines in N* droplets, are in progress and will be published elsewhere.

S. Ž. acknowledges partial support from the Science and Technology Center ALCOM under grant DMR 89-20147.

References

[1] CLADIS, P. E., WHITE, A. E., and BRINKMAN, W. F., 1979, *J. Phys., Paris*, **40,** 325.
[2] YANG, D. K., and CROOKER, P. P., 1991, *Liq. Crystals*, **9,** 245.
[3] QUIGLEY, J. R., and BENTON, W. J., 1977, *Molec. Crystals liq. Crystals*, **42,** 43.
[4] VOLOVIK, G. E., and MINEEV, V. L., 1977, *Zh. eksp. teor. Fiz.*, **72,** 2256.
[5] KLÉMAN, M., 1981, *Points, Lines and Walls* (Wiley), pp. 82–83, 273.
[6] DE GENNES, P. G., 1974, *The Physics of Liquid Crystals* (Oxford University Press), p. 264.
[7] CLADIS, P. E., and KLÉMAN, M. J., 1972, *J. Phys., Paris*, **33,** 591.
[8] MERMIN, N. and D., 1979, *Rev. mod. Phys.*, **51,** 591, 594, 596, 638, 641.
[9] RAULT, J., 1972, *J. Phys., Paris*, **33,** 383.
[10] RAULT, J., 1974, *Phil. Mag.*, **29,** 621.
[11] CHANDRASEKHAR, S., 1986, *Adv. Phys.*, **35,** 507, 511–513.
[12] TOULOUSE, G., and KLÉMAN, M., 1976, *J. Phys. Paris*, **37,** 149.
[13] VOLOVIK, G. E., 1978, *Pis'ma Zh. éksp. teor. Fiz.*, **28,** 65.
[14] VOLOVIK, G. E., and LAVRENTOVICH, O. D., 1983, *Zh. éksp. teor. Fiz.*, **85,** 1997.
[15] CLARK, N. A., and RIEKER, T. P., 1988, *Phys. Rev.* A, **37,** 1053.
[16] ŽUMER, S., KRALJ, S., and BEZIČ, J., 1992, *Molec. Crystals liq. Crystals*, **212,** 163.
[17] BEZIĆ, J., and ŽUMER, S., 1992, *Liq. Crystals*, **11,** 593.
[18] BOULIGAND, Y., and LIVOLANT, F., 1984, *J. Phys., Paris*, **45,** 1899.